RASĀYAN *J. Chem.*
Vol. 18 | No. 3 |1704-1716| July-September | 2025
ISSN: 0974-1496 | e-ISSN: 0976-0083 | CODEN: RJCABP
http://www.rasayanjournal.com
http://www.rasayanjournal.co.in

STUDY OF REDOX POTENCY OF COPPER OXIDE NANOPARTICLES IN THE OXIDATION OF VILAZODONE HYDROCHLORIDE WITH OXIDANT CHLORAMINE-T: A KINETIC AND MECHANISTIC INVESTIGATION

K. M. Vidyashree[1], M. K. Arpitha[2], H. S. Sonakshi[3] and H. P. Jayadevappa[4,✉]
Department of Chemistry, Yuvaraja's College, University of Mysore,
Mysuru-570006, Karnataka, India
✉Corresponding author: hpjayadevappa@gmail.com

ABSTRACT

In this research, Copper oxide nanoparticles were chemically prepared and investigated for their potency as a catalyst for the kinetic, mechanistic, and thermodynamic study of the oxidation of vilazodone hydrochloride (VLH) using chloramine-T in Hydrochloric acid medium was performed at 303K. The prepared nanoparticles were subjected to scanning electron microscopy (SEM) to study the morphological features, to structural analysis by X-Ray diffraction (XRD), and for composition of metal oxides by energy-dispersive X-ray spectroscopy (EDX). Oxidant followed first-order dependence in both the copper oxide-catalyzed and uncatalyzed reactions. The reaction rate showed a fractional-order dependence on [H^+], as revealed by kinetic analysis, and on [VLH] concentration. The order followed by the catalyst copper oxide nanoparticle was fractional. The reaction products were identified. The stoichiometry of the reaction was found to be 1:1 in both cases. The rate of a reaction remained unchanged for halide ions in both cases. Spot testing was used to identify the oxidation products. Ionic strength had a negligible effect in both cases. Thermodynamic parameters were computed. The kinetic law was formulated by considering the reaction pathways.

Keywords: Vilazodone hydrochloride, Copper Oxide nanoparticle, Kinetics, Chloramine-T, Oxidation, SEM, XRD.
RASĀYAN*J. Chem.*, Vol. 18, No.3, 2025

INTRODUCTION

In today's world, nanoparticles have numerous applications. Researchers are exploring new uses for nanoparticles. Because of its exceptionally small size and high surface area relative to its volume, they exhibit unique chemical, physical, and biological characteristics. Nanoparticles can potentially be composed of various materials that include metals, ceramics, and biomolecules. Currently, metal oxides, metals, ceramic silicates, and polymer nanoparticles have been prepared and have many potential applications.[1,2]Copper nanoparticles exhibit promising applications in diverse fields, including electronics, optics, and medicine, and the manufacture of lubricants, Nano-fluids, conductive films, and antimicrobial agents.[3,4] Nanoparticles of Copper oxide were prepared at a low cost by the sol-gel method[5], Chemical Co-Precipitation method[6], Hydro-thermal method[7], Green synthesis,[8] and Biosynthesis method.[9]

Vilazodone Hydrochloride (VLH) is named as 5-[4-(5-cyano-1H-indol-3-yl) butyl] piperazine-1-yl] benzofuran-2-carboxamide hydrochloride. It received FDA (Food and Drug Administration) approval in January 2011 for Major Depressive Disorder (MDD) treatment. Vilazodone hydrochloride is one of the novel dual-acting serotonergic antidepressants that binds the effect of an SSRI (Selective Serotonin Reuptake Inhibitor)with 5-HT_{1A}-receptor partial agonist activity. It is observed to improve anxiety symptoms in patients and maintains a consistent response among patients with major clinical depression.[10-13]

Sodium-N-chloro-4-methylbenzenesulfonamide, widely known as Chloramine-T (CAT), is a potent N-halogenated amine compound. It is a mild, effective, stable, inexpensive, and non-toxic mild oxidizing agent. It is a versatile oxidizing agent with diverse applications. CAT displays diverse kinetic behavior, resulting from the pH-dependent formation of various oxidizing species. The oxidation-reduction potential

http://doi.org/10.31788/RJC.2025.1839230
This work is licensed under a CC BY 4.0 license.

of CAT exhibits a pH-dependent decrease.[14-16] The Kinetic, mechanistic, and thermodynamic aspects of many of its redox reactions weredocumented.[17-19]A literature review revealed that only pharmacological, clinical, and spectrophotometric methods for Vilazodone hydrochloride have been reported.[20-22] A kinetic and mechanistic investigation of copper oxide nanoparticle catalyzed and uncatalyzed oxidation of Vilazodone hydrochloride by CAT was not reported.In this manuscript, we report a kinetic, mechanistic, and thermodynamic study of the copper oxide nanoparticle-catalyzed and uncatalyzed oxidation of Vilazodone hydrochloride using Chloramine-T in a medium containing Hydrochloric acid medium.

EXPERIMENTAL

Materials and Methodology

Copper oxide nanoparticles were prepared using copper chloride salt by the sol-gel method, as reported by Hadeel K. Thanoon *etal.* To the stirred solution of 0.2M $CuCl_2.2H_2O$, 1ml of glacial acetic acid is added, and then the solution is heated nearly to 100 ºC and NaOH solution is added to the stirred mixture to maintain a pH of 7. The Color of the solution transforms from green to black, and a black precipitate forms immediately. Wash the precipitate with de-ionized water several times and dry it at room temperature. A fresh solution of VLH was made for each experiment by dissolving the necessary amount of VLH in deionized water. Deionized water was used to prepare an aqueous CAT (E. Merck), and its strength was determined by iodometric titration. And to prevent photochemical deterioration and the solution was stored in a brown glass bottle in the dark. Copper chloride salt was used to prepare the Copper oxide nanoparticles via a sol-gel method. A solution of copper oxide was prepared using doubly distilled water. For the remaining work, analytical-grade solutions were utilized, and their solutions had been freshly prepared using double-deionized water. Methyl alcohol was used to alter the dielectric constant. The solution of Hydrochloric acid is used to examine the effect of acid concentration. To study the impact of halide concentration, a sodium chloride solution was introduced. Sodium perchlorate solution was used to ensure a constant ionic strength throughout the reaction.

Kinetic Measurements

Kinetic study of the oxidation process between VLH and Chloramine-T was performed under conditions of pseudo-first-order kinetics $[VLH]_0 >> [CAT]_0$ in copper oxide nanoparticle catalyzed and also in uncatalyzed reactions. The progress of the CuO nanoparticle catalyzed and uncatalyzed oxidation reaction was examined by evaluating the reduction in the maximum absorbance for oxidant CAT (λ_{max}=260nm). Absorbance values of all the reactions were measured and recorded on a spectrophotometer (ThermoScientific), Instrument model GENESYS 150 (Fig.-1).

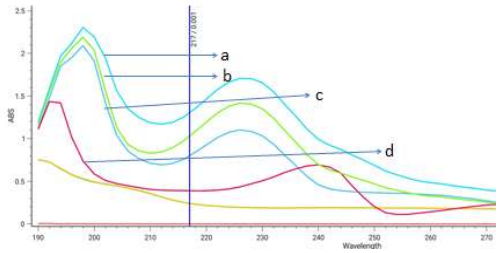

Fig.-1: UV-VisibleSpectral Analysis for Various Reactant Combinations.
(a) CAT, (b) CAT + CuO + VLH +Cl^-+ H^+, (c) CuO + VLH + Cl^-+ H^+,(d)CAT + VLH + Cl^-+ H^+

The kinetic runs were conducted at 30±0.1ºC. The reaction mixture, containing the necessary amounts of solutions of VLH, HCl and NaCl along with double-distilled water to maintain a consistent volume (100ml) for all different kinetic runs, was kept at a constant temperature of 303K. In a separate reagent bottle, the CAT solution was maintained at an identical temperature. An accurately measured volume of pre-equilibrated CAT solution was introduced into the reaction mixture, and the resulting mixture was thoroughly homogenized. The course of the reaction was carefully observed and monitored through regular withdrawing aliquots (5ml) of the reaction mixture by estimating unreacted CAT iodometrically for uncatalyzed reaction. The catalyzed reaction was studied by mixing CAT with VLH, which contains HCl, NaCl, and Copper oxide solution. To investigate the reaction's course, measurements were taken at

different time intervals. Rate constants for the Pseudo-first order reaction for Nano particle catalytic (k_C) and uncatalytic (k_U) reactions were evaluated based on the linearity plots of log [CAT] against time were repetitive within ±2%.The rate constant for the pseudo-first-order reaction was investigated in every condition by plotting a graph of absorbance versus time, throughout three half-lives. It retains a linear shape. The observed rate constant is independent of the chloramine-T concentration under pseudo-first-order conditions.

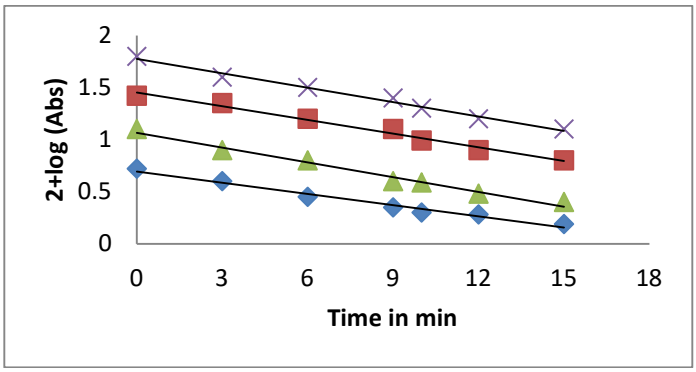

Fig.-2: Pseudo-First-Order Plots for different Concentrations of CAT

Stoichiometry and Product Validation

The kinetic reaction solution contained one molar quantity of VLH and one molarquantity of CAT in the presence of HCl, NaCl in an uncatalyzed reaction, and copper oxide in a Nano-catalyzed reaction was equilibrated under stirred conditions at 303K for about 24 hours. Unreacted oxidant (CAT) was estimated iodometrically using starch as an indicator. The results support a stoichiometric ratio of 1:1 between substrate and oxidant, as shown below,

$$C_{26}H_{27}N_5O_2+PTSO_2NClNa+H_2O \xrightarrow{CuO} C_{13}H_{12}N_2O + C_{13}H_{15}N_3O_2+PTSO_2NH_2+ HCl + Na^+ +H^+$$

Where PT = $CH_3C_6H_4$ (1)

Once the reaction had finished, the product was extracted using diethyl ether. The ether layer contained oxidation products of substrate VLH,3-(4-oxobutyl)-1H-indole-5-carbonitrileand 5-(piperazin-1-yl)benzofuran-2-carboxamide, which were extracted with aqueous sodium hydroxide solution and identified via TLC spot test and product confirmed by Tollen's reagent test and alkaline hydrolysis, respectively. The product formed through reduction was Para-Toluene Sulfonamide, was isolated via ethylacetate extract ion and identified using TLC.

RESULTS AND CONCLUSION

Scanning Electron Microscopy (SEM)

SEM characterization revealed the surface morphology of the nanoparticles. Figure-3 represents a scanning electron microscopy image of the synthesized copper oxide nanoparticle.

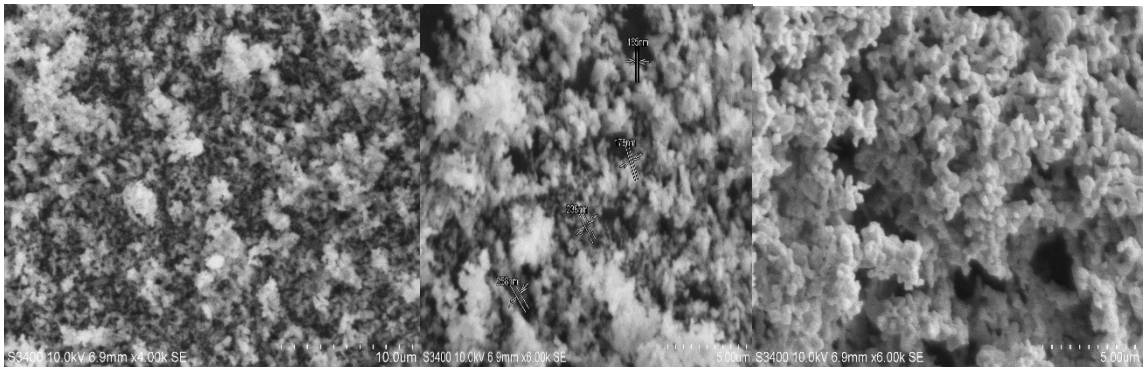

Fig.-3: SEM images of CuO Nanoparticles

Energy-Dispersive X-ray Spectroscopy (EDAX)

EDAX is a technique that was utilized to determine the elemental composition of nanoparticles. The EDAX spectrum of the synthesized copper oxide nanoparticle is shown in Fig.-4.

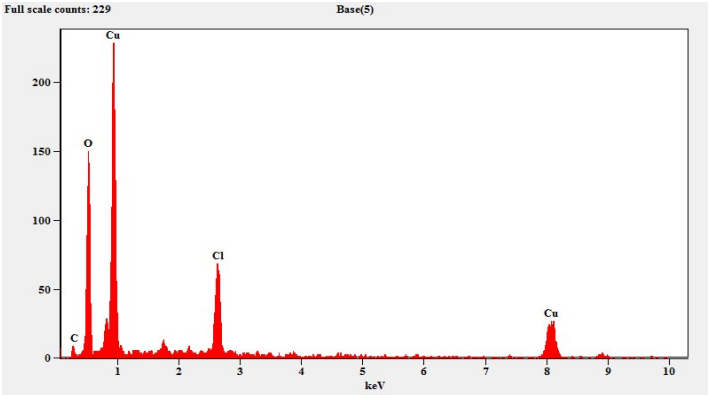

Fig.-4: EDAX image of CuO Nanoparticle

X-ray Diffraction (XRD)

The technique of XRD is employed to study the crystal structure and phase composition of nanoparticles. Figure-5 shows the XRD pattern of the nanoparticle copper oxide.

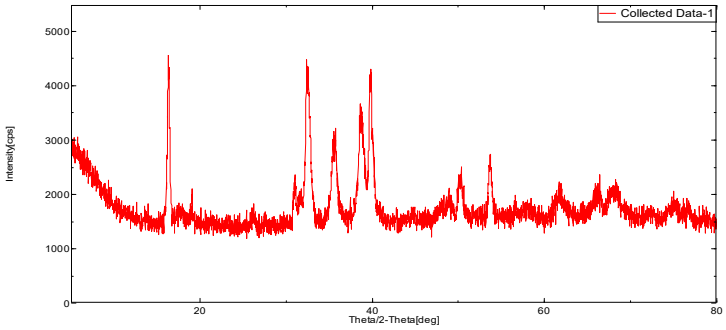

Fig.-5: XRD Image of Copper Oxide Nanoparticle

Reactants Concentration Effect onthe Rateof a Reaction

Reaction studied under Pseudo-first order kinetics, that is [Substrate] >> [oxidant] by varying the concentration of CAT at constant temperature and at constant [VLH],[HCl], [NaCl], and CuO solutions. The log [oxidant] against time plots exhibited a linear relationship, indicating that the rate followsfirst-order kinetics dependent on oxidant concentration in the absence and presence of Nano-catalyst. From the linear plots, pseudo-first-order rate constants were readily determined (Table-1). The invariance of the rate constant k_C / k_U with changing oxidant concentration provides additional evidence for the first-order kinetics of the reaction rate on [CAT]. With identical conditions and experimental parameters, the concentration of VLH was varied, and the rate constants for both catalyzed and uncatalyzed reactions increased with increasing concentration of VLH (Table-1). The linearity graph of log k_C / log k_U against log [VLH] (Fig.-6), having a slope of 0.53 for un-catalyzed reaction, indicates fractional-order dependence on [VLH], and the Nano-catalyzed reaction indicates fractional-order dependence on [VLH] with a slope of 0.57. The rate constants k_C/ k_U were calculated, and details are summarized in Table-1.

Influence of Acid Concentration

The kinetic study was conducted by varying [HCl] while maintaining all other reaction parameters constant. Reaction rate increased with HCl concentration (Table-1) for both Nano-catalyzed and uncatalyzed reactions. Graph of log k_C / log k_U v/s log $[H^+]$ (Fig.-7) was linear with a positive slope of 0.42 and 0.65 for un-catalyzed and copper oxide nano-catalyzed reactions, respectively, showing fractional reaction order dependence on $[H^+]$.

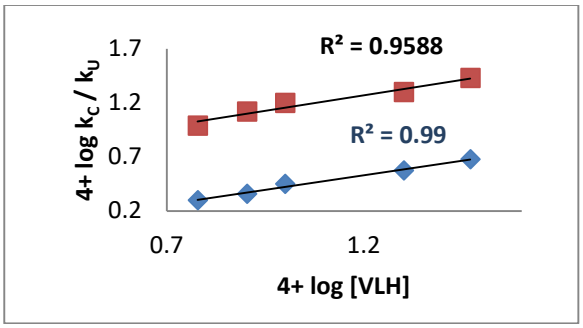

Fig.-6: Graph of log k_U / k_C against log [VLH]

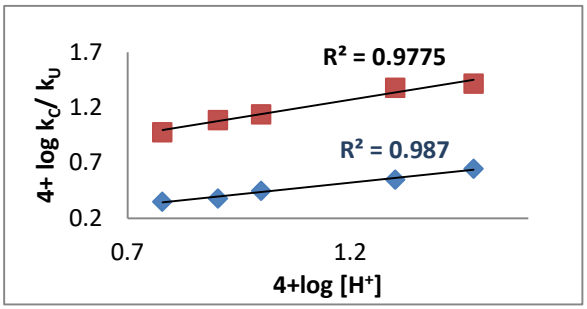

Fig.-7: plots of log k_u / k_c versus log [H^+]

Influence of Halide Ions on Rate

The variation in chloride ion concentration on reaction rate for both cases was examined by altering the amount of NaCl solution at constant [CAT], [VLH], HCl, CuO, and temperature. The rate of Nano-catalyzed and uncatalyzed reactions increased with the increasing concentration of NaCl solution (Table-1). Graph of log k_c / log k_u against log [Cl^-] (Fig.-8) showed a linear relationship with a slope of 0.36 and 0.37 for un-catalyzed and Nano-catalyzed reactions, respectively, confirming fractional order dependence on halide ions.

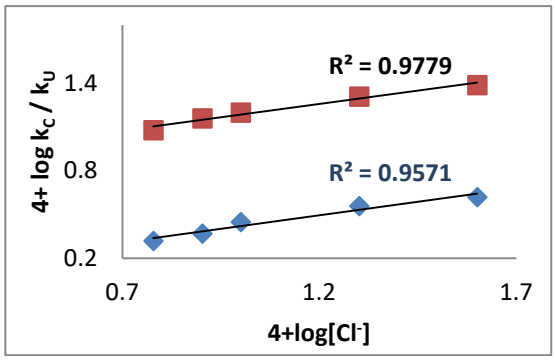

Fig.-8: Graph of log k_U / k_C against log [Cl^-]

Influence of Ionic Strength

The ion concentration of the reaction medium was altered by adding $NaClO_4$ (0.1-1.0 mol /dm^3). The constancy of the reaction rate indicated that nonionic species play a crucial role in the rate-determining steps of both Nano-catalyzed and non-catalyzed reactions.

Influence of Dielectric Constant

The impact of dielectric constant on the reaction was examined by modifying the solvent composition with varying proportions ofmethyl alcohol (0-30%,v/v). For both reactions, it was found that higher dielectric permittivity (D) of the medium resulted in lower reaction rates (Table-2). The graph of logk_C / log k_U against 1/D (D is a dielectric permittivity) exhibited a linear dependence with a negative slope(Fig.-9).

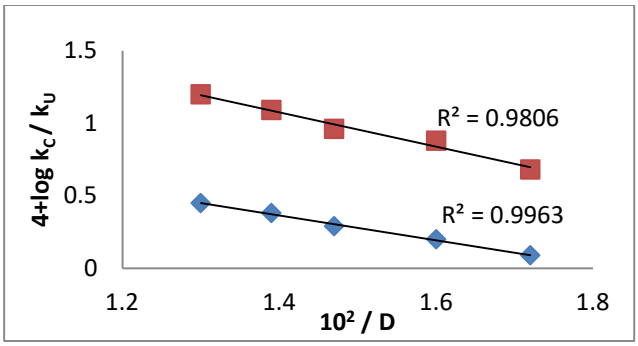

Fig.-9: Graph of log k_C/ k_U versus $10^{2}/D$

Table-1: Influence of [CAT], [VLH], $[H^+]$, $[Cl^-]$, and [CuO] on rate studied at 303K for Nanoparticle Catalyzed Oxidation of VLH with Oxidant Chloramine-T in Hydrochloric Acid Media.

$10^5\times$ [CAT] mol /dm^3	$10^5\times$ [VLH] mol /dm^3	$10^4\times$ $[H^+]$ mol /dm^3	$10^4\times$ $[Cl^-]$ mol /dm^3	$10^6\times$ [CuO] mol /dm^3	$10^4\times k_U$ Sec^{-1}	$10^3\times k_C$ Sec^{-1}
6	10	10	10	10	2.85	1.588
8	10	10	10	10	2.86	1.587
10	10	10	10	10	2.85	1.588
20	10	10	10	10	2.85	1.587
30	10	10	10	10	2.86	1.587
10	6	10	10	10	2.01	0.987
10	8	10	10	10	2.29	1.325
10	10	10	10	10	2.85	1.588
10	20	10	10	10	3.75	2.013
10	30	10	10	10	4.80	2.698
10	10	6	10	10	2.26	0.961
10	10	8	10	10	2.40	1.254
10	10	10	10	10	2.85	1.588
10	10	20	10	10	3.55	2.397
10	10	30	10	10	4.50	2.653
10	10	10	6	10	2.12	1.225
10	10	10	8	10	2.35	1.469
10	10	10	10	10	2.85	1.588
10	10	10	20	10	3.68	2.065
10	10	10	40	10	4.23	2.469
10	10	10	10	6	-	1.209
10	10	10	10	8	-	1.335
10	10	10	10	10	-	1.588
10	10	10	10	20	-	2.048
10	10	10	10	30	-	2.263

T=303K,10^2/D=1.2

Influence of the Reduction Product PTS Concentration on the Rate

Adding Para-touleneSulphonamide (1×10^{-3} -10×10^{-3} mol /dm^3), the rate remained largely unaffected by the reduced form of the oxidant. This suggests that it does not participate in the pre-equilibrium step, both in Nano-catalyzed and uncatalyzed reactions.

Influence of Nano Catalyst CuO on the Rate

The concentration gradient of catalyst CuO was changed in the reaction mixture while maintaining constant [VLH], [HCl], [CAT], $[Cl^-]$, and temperature. As the CuO concentration increased, the rate also increased accordingly from 8×10^{-6} to 40 $\times10^{-6}$. A fractional order dependence on the catalyst was

observed with a positive slope of 0.39 from the linearity plot of log k_C versus log [CuO] (Fig.-10).

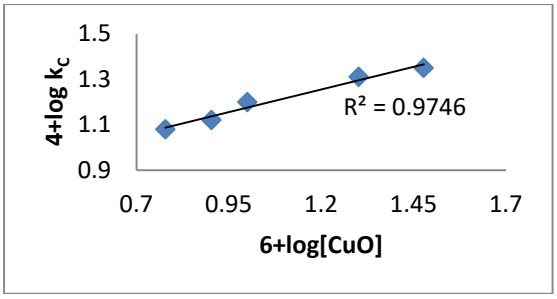

Fig.-10: Plots of log k_C versus log [CuO]

Influence ofTemperature

The temperature dependence of the kinetic reaction was examined by carrying out experiments over a range of temperatures (293K-313K), keeping the reaction experimental conditions constant. It showed that a direct relationship exists between temperature and rate constant for both Nano-catalyzed and uncatalyzed reactions. The reaction kinetic parameters were calculated from a linear Arrhenius graph of log k_C / log k_U against1/T (Fig.-11), and their values and rate constant are summarized in Table-3.

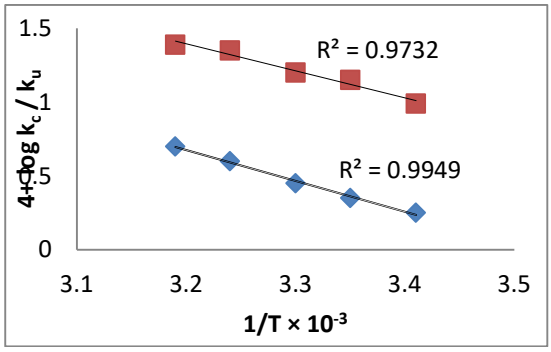

Fig.-11: Graph of log k_C / k_U versus 1/T

Table-3: Temperature Effect and Kinetic Parameters

Temperature in K	$k_c \times 10^4$ sec^{-1}	$k_u \times 10^4$ sec^{-1}	Activation parameters	Nano catalyzed	Un-catalyzed
293	5.82	1.81	E_a(kJ mol^{-1})	34.84	40.01
298	9.65	2.32	$\Delta H^{\neq}$ (kJ mol^{-1})	32.32	37.49
303	15.88	2.85	$\Delta S^{\neq}$ (kJ mol^{-1})	-172.82	-189.12
308	20.01	4.02	$\Delta G^{\neq}$ (kJ mol^{-1})	84.44	94.80
313	30.99	5.92	logA	3.2	3.35

Detection of Free Radical Species

Initiation of polymerization in aqueous acrylamide is not achieved with the kinetic reaction mixture. It shows the Non-involvement of free radical reactive species in the Nano-catalyzed and uncatalyzed course of the reaction.

Catalytic Activity

Under conditions of a catalyst, both the Nano-catalyzed and uncatalyzed reactions occur concurrently, the catalyst increasing the rate of reaction by providing a more energetically favorable pathway, as proposed by Moelwyn-Hughes.[23]

That is,

$$k_c = k_u + K_C [Cu (II)]^x, \quad (2)$$

Here, k_c signifies the rate constant for Nano-catalyzed reaction, $k_u$refers to the rate constant of the uncatalyzed reaction, K_C signifies the catalytic activity concerning Cu (II) catalyst. 'x' signifies the order of the catalyst Cu (II). Equation (2) enables the evaluation of K_C values over a wide range of temperatures

and is summarized in Table-4.

The kinetic variables were determined by constructing an Arrhenius graph of log k_c / k_u concerning 1/T, allowing for the calculation of K_C values. The variation in kinetic parameters between the nano-catalyzed and uncatalyzed reactions elucidates the significant impact of the Cu (II) on the reaction. Complex formation occurs between substrate Vilazodone hydrochloride and catalyst copper oxide, indicating that the nano-catalyst copper exhibits a more reducing character than Vilazodone hydrochloride by itself. As a result, Cu (II) facilitates a change in the reaction pathway by reducing its energy of activation energy.

Table-4: Values of the Catalytic Constant (K_C) and Kinetic Variables

Temperature (K)	$K_C \times 10^3$	Kinetic Variables	Values
293	5.98	E_a(kJ /mol)	57.44
298	10.94	$\Delta H^{\neq}$ (kJ /mol)	54.92
303	19.4	$\Delta S^{\neq}$ (kJ /mol)	-19.57
308	23.8	$\Delta G^{\neq}$ (kJ /mol)	60.85
313	37.4	logA	11.90

Rate Law and Mechanism

Mechanism for Uncatalyzed Kinetic Reaction

Chloramine-T exhibits weak oxidizing properties in both alkaline and acidic media, facilitating a Bi-electron transfer to generate products. In aqueous solution, it displays strong electrolytic properties, but in acidic aqueous media, it undergoes the following equilibria, resulting in various ionized species.[24-27]

$$CH_3C_6H_4SO_2NClNa \rightleftharpoons CH_3C_6H_4SO_2NCl^- + Na^+ \quad (3)$$

$$CH_3C_6H_4SO_2NCl^- + H^+ \rightleftharpoons CH_3C_6H_4SO_2NHCl \quad (4)$$

$$2CH_3C_6H_4SO_2NHCl \rightleftharpoons CH_3C_6H_4SO_2NH_2 + CH_3C_6H_4SO_2NCl_2 \quad (5)$$

$$CH_3C_6H_4SO_2NCl_2 + H_2O \rightleftharpoons CH_3C_6H_4SO_2NHCl + HOCl \quad (6)$$

$$CH_3C_6H_4SO_2NHCl + H_2O \rightleftharpoons CH_3C_6H_4SO_2NH_2 + HOCl \quad (7)$$

Thus, in an aqueous mixture, CAT can generate various oxidative species, including $CH_3C_6H_4SO_2NHCl$,$CH_3C_6H_4SO_2NCl_2$,and HOCl. The absence of second-order kinetics concerning oxidant suggests that $CH_3C_6H_4SO_2NCl_2$is not a reactive species. Furthermore, the rate is not decreased by the addition of PTS. Thus, HOCl is not the main reactant in the oxidation reaction.Therefore,$CH_3C_6H_4SO_2NHCl$is regardedasthe primaryactiveoxidizingspecies.Inacidic media(pH<2),$CH_3C_6H_4SO_2NHCl$ undergoes protonation to form $CH_3C_6H_4SO_2NH_2Cl^+$.[28]

$$CH_3C_6H_4SO_2NHCl + H^+ \rightleftharpoons CH_3C_6H_4SO_2NH_2\overset{\oplus}{Cl} \quad (8)$$

Scheme-1 illustrates a proposed mechanism that accounts for the experimental results obtained during VLH oxidation using CAT. In scheme-1, $CH_3C_6H_4SO_2NHCl$ signifies the reactive oxygen species, VLH corresponds to the substrate, X and X^1 represent the intermediate complex active species. The reaction is started via the generation of $CH_3C_6H_4SO_2NH_2Cl^+$ ion. It reacts with the VLH molecule to give intermediate complex X. Intermediate X, on dissociation to give complex X^1 in rate rate-determining step with the elimination of HCl. The complex $X^{1,}$ on reaction with water, gives products. Reaction mechanism illustrated in Scheme-1.

Shown in Scheme-1, X and $X^{'}$ are denoted complex active species, as predicted in Scheme-2, their structures are as follows:

Let $[CAT]_t$ be the overall strength of CAT, then

$[CAT]_t = [PTSO_2NH_2Cl^+] + [PTSO_2NHCl] + [X]$ (1.1)
Where, PT = $CH_3C_6H_4$

Based on reaction steps (i) and (ii) from Scheme-1,
$[PTSO_2NH_2Cl^+] = \frac{[X]}{k_2[VLH]}$ (1.2)

$[PTSO_2NHCl] = \frac{[X]}{k_1k_2[VLH][H^+]}$ (1.3)

Upon substituting equations (1.2) and (1.3) in equation (1.1) and solving for [X], we obtain,
$[X] = \frac{k_1k_2[H^+][VLH][CAT_t]}{1+k_1[H^+]+ k_1k_2[H^+][VLH]}$ (1.4)

As indicated by the slowest step of Scheme-1,
Rate = k_3 [x] (1.5)

From equation (1.5), substituting for [X] in equation (1.4), we get,
Rate = $\frac{k_1k_2k_3[H^+][VLH][CAT]_t}{1+k_1[H^+]+k_1k_2[H^+][VLH]}$ (1.6)
The derived rate law successfully reproduces the experimental findings, including fractional-order dependence on [VLH], [H^+], and the kinetics of the reaction is first-order in [CAT].
Since Rate = $k_u[CAT]_t$, equation (1.6) can be rearranged to give,

$K_u = \frac{k_1k_2k_3[H^+][VLH]}{1+k_1[H^+]+k_1k_2[H^+][VLH]}$ (1.7)

On rearranging equation (1.7), we get,
$\frac{1}{k_u} = \frac{1}{k_2k_3[VLH]}\{\frac{1}{k_1[H^+]} + 1\} + \frac{1}{k_3}$ (1.8)

Graph of$1/k_u$ versus 1/[VLH], constructed from equations 1.7 and 1.8, yields straight lines, enabling the calculations of rate constantsk_1, k_2,and k_3 from the slope and intercept values. Changing the proportions of methyl alcohol (0-40% v/v) altered the dielectric constant of the medium. The negative slope of the log k' against 1/D graph indicates the occurrence of dipole-dipole interaction force in the reaction. The PTS (*p*-Toulenesulphonamide) fails to change the reaction rate in this work, indicating its absence in a pre-equilibrium step. The rate is independent of ionic strength, which suggests that non-ionic species play a crucial role in the slow step. Halide ion has a slightly positive effect on the rate. The calculated kinetic parameters provide strong evidence in support of the proposed mechanism. Moderate activation energies provide strong observations for the derived mechanism and are associated with the derived rate law. The relatively higher positive values of Gibbs free energy and enthalpy indicate that the transition state is extensively hydrated, and a high negative value of entropy suggests that the formation of an ordered associative transition state involves a reduction in degrees of freedom.

Mechanism for Nano-Catalyzed Reaction
The copper oxide nanoparticle catalyzed reaction of VLH by CAT in HCl medium exhibits similar stoichiometry to the uncatalyzed reaction. The reaction exhibited first-order kinetics for oxidant CAT. Fractional-order was foundfor both VLH and HCl. An increase in catalyst concentration was found to enhance the reaction rate. The order of reaction for the catalyst CuO is fractional order. The dielectric constant of the medium was examined by varying the concentration of Methyl alcohol.The dielectric constant has a slightly negative effect. $NaClO_4$ is added to the reaction mixture to assess the effect of ionic strength. No significant impact of ionic strength on the rate of a reaction, which suggests the participation of non-ionic species in the kinetic reaction. In Copper oxide nanoparticle catalyzed oxidation of VLH requires one mole of CAT to oxidize one mole of VLH, confirming that 1:1 stoichiometry. On the basis previous discussion, a proposed mechanism is outlined in the following Scheme-3.

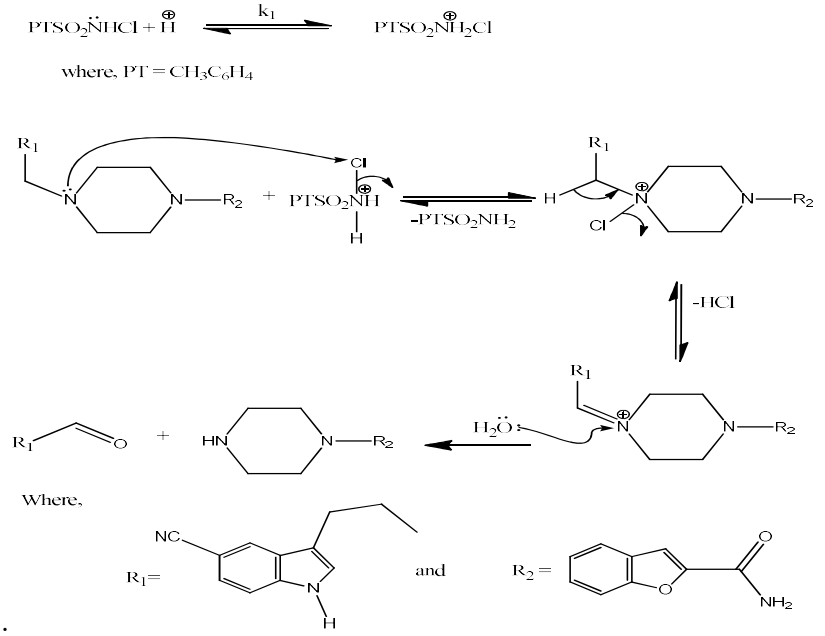

Scheme-2

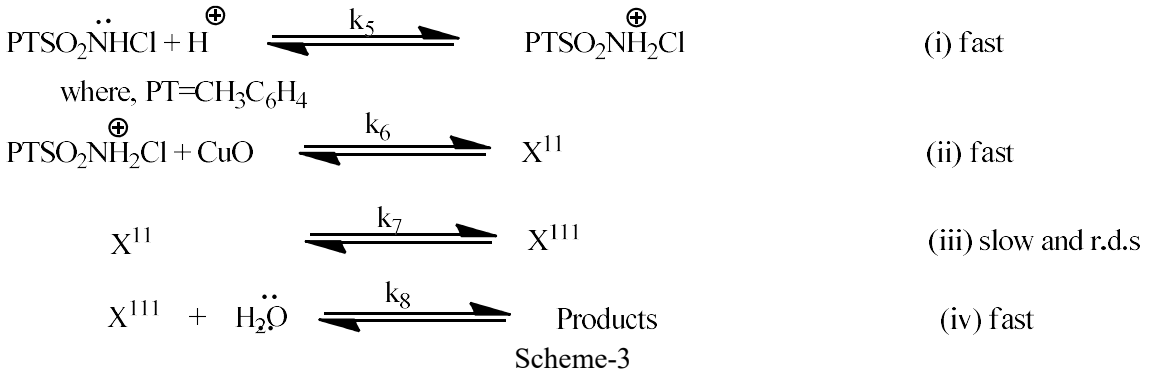

Scheme-3

As shown inScheme-3, X" and X"' are complex intermediates, and their structures are illustrated in Scheme-4.

Let $[CAT]_t$be the overall effective concentration of the oxidant CAT, then

$$[CAT]_t = [PTSO_2NH_2Cl^+] + [PTSO_2NHCl] + [X''] \quad (3.1)$$

From Scheme-3 of steps (i) and (ii),

$$[PTSO_2NH_2\,Cl^+] = \frac{[X'']}{k_6[CuO]} \quad (3.2)$$

$$[PTSO_2NHCl] = \frac{[X'']}{k_5k_6[CuO][H^+]} \quad (3.3)$$

Upon substituting equations (3.2) and (3.3) into equation (3.1) and solving [X"], we obtain

$$[X''] = \frac{k_5k_6[H^+][CuO][CAT]_t}{1+k_5[H^+]+k_5k_6[H^+][CuO]} \quad (3.4)$$

From rate rate-determining step of Scheme-3,

$$\text{Rate} = k_7\,[x''] \quad (3.5)$$

By putting [X"], from equation (3.5) to equation (3.4), we get

$$\text{Rate} = \frac{k_5 k_6 k_7 [H^+][CuO][CAT]_t}{1+k_5[H^+]+k_5 k_6 [H^+][CuO]} \quad (3.6)$$

The derived rate law was reliable with experimental observations. The results indicate a first-order kinetic dependence on [CAT] and fractional-order kinetic dependences on [VLH], [H^+], and [CuO] concerning the reaction rate.

As Rate = $k_C[CAT]_t$, equation (3.6) can be modified into,

$$\text{Rate} = \frac{k_5 k_6 k_7 [H^+][CuO]}{1+k_5[H^+]+k_5 k_6 [H^+][VLH]} \quad (3.7)$$

On rearranging equation (3.7), we get,

$$\frac{1}{k_c} = \frac{1}{k_7}\left\{\frac{1}{k_6[CuO]}\left(\frac{1}{k_5[H^+]} + 1\right) + 1\right\} \quad (3.8)$$

From equations (3.7) and (3.8), straight lines were obtained for a graph of $1/k_c$ against 1/[VLH]. Values for the rate constantsk_5, k_6,and k_7 were obtained by analyzing the slope and intercept.

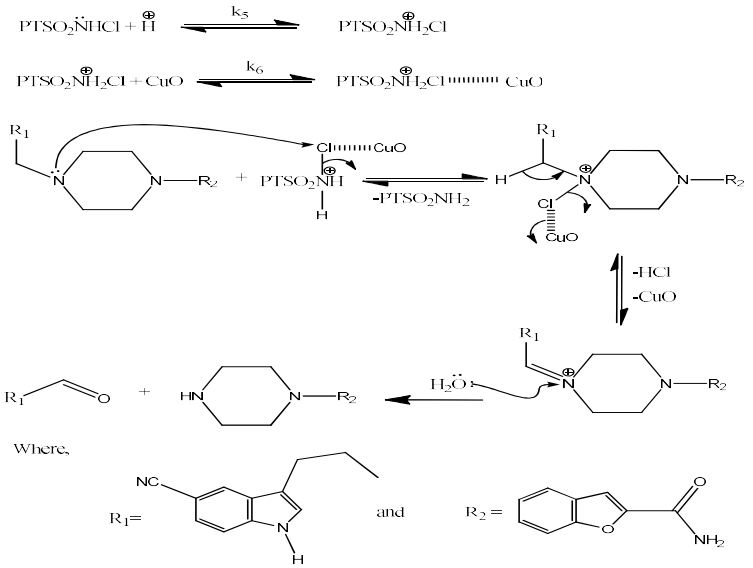

Scheme-4

CONCLUSION

The Copper oxide nanoparticle catalyzed and uncatalyzed oxidation of the CAT-VLH oxidation-reduction reaction was studied in acidic medium using HCl. A 1:1(equation 1) stoichiometric ratio has been determined for the oxidation reaction between VLH and CAT in both copper oxide Nanoparticles catalyzed and uncatalyzed conditions. The impact of halide ions, the impact of acid concentration, the impact of catalyst, the impact of oxidant, the impact of substrate, the influence of ionic strength, the influence of temperature, and the influence of dielectric constant on the kinetic reaction was investigated. The kinetic parameters $\Delta G^{\neq}$, $\Delta H^{\neq}$, $\Delta s^{\neq}$, and E_a were determined from the linear Arrhenius plots using the observed data. A mechanism is suggested that is consistent with the observed kinetics, and the rate law was successfully derived using kinetic data.

ACKNOWLEDGEMENTS

The Authors acknowledge the resources and facilities given by the University of Mysore, Mysuru, specifically at Yuvaraja College, which enabled them to complete this kinetic research.
Xc vbnm/.,mn bvcxsa=-o09876=[

CONFLICT OF INTERESTS

The authors declare that there is no conflict of interest.

AUTHOR CONTRIBUTIONS

The present work is related to *SDG-12: Responsible Consumption and Production.* All the authors contributed significantly to this manuscript, participated in editing/ reviewing, and approved the final draft for publication. The research profile of the authors can be verified from their ORCID ids, given below:

K. M. Vidyashree https://orcid.org/0009-0009-8151-8015
M. K. Arpitha https://orcid.org/0009-0007-4983-1701
H.S. Sonakshi https://orcid.org/0009-0007-1500-0758
H.P. Jayadevappa https://orcid.org/0000-0003-4925-7782

Open Access: This article is distributed under the terms of the Creative Commons Attribution 4.0 International License (http://creativecommons.org/licenses/by/4.0/), which permits unrestricted use, distribution, and reproduction in any medium, provided you give appropriate credit to the original author(s) and the source, provide a link to the Creative Commons license, and indicate if changes were made.

REFERENCES

1. A. M. Awwad, Nida M. Salem A. O. Abdeen, *Nanoscience and Nanotechnology,* **2**, 164(2012), https://doi.org/10.5923/j.nn.20120206.03
2. G. Mustafa, H. Tahir, M. Sultan, N. Akhtar, *African Journal of Biotechnology,***12**, 6650(2013), https://doi.org/10.5897/AJB2013.13058
3. Luis. M Liz-Marzan, I. M. Isabel Lado-Turnio, *Langmuir,* **12**, 3586(1996), https://doi.org/10.1021/la951501e
4. Kirti Patel, Sudhir Kapoor, D.P. Dave, Tulsi Mukherjee, *Journal of Chemical Science*, **117**, 53(2005), https://doi.org/10.1007/BF02704361
5. Hadeel K. Thanoon, Kadhim A. Hubeatir, Ahmed A. AI-Amiery, *International Journal of Research in Engineering and Innovation*, **1,** 44(2017)
6. Willington Marques Rangel, Rozineide A. Antunes Boca Santa, Humberto Gracher Riella, *Journal of Material Research and Technology,* **9**, 995(2020), https://doi.org/10.1016/j.jmrt.2019.11.039
7. Kondaiah Seku, Bhagavanth Reddy Ganapuram, Babu Pejjai, Girija MangatayaruKotu, Narasimha Golla, *International Journal of Nano Dimension*, **9,** 9(2018), https://dorl.net/dor/20.1001.1.20088868.2018.9.1.2.6
8. Nilanjan Chakraborty, Jishnu Banerjee, Pallab Chakraborty, Anuron Banerjee Sumeddha, Kasturi Ray, Krishnanenduacharaya, Joy Sarkar, *Green Chemistry Letters and Reviews*, **15**, 189(2022), https://doi.org/10.1080/17518253.2022.2025916
9. Navid Rabiee, Mojtaba Bangherzadeh, Masha Kiani, Amir Mohammad Ghadiri, Fatemeh Etessamifar, Amir Hossein Jaberizadeh and Alireza Shakeri, *International Journal of Nanomedicine*, **15**, 3984(2020), https://doi.org/10.2147/IJN.S255398
10. Maryadele J. O'Neil, *Journal of Chemical Information and Modeling*, **47,** 703(2007), https://doi.org/10.1021/ci700022n
11. M. D Rachna Kalia, Moneeshindra S. Mittal, M. D Sheldon H. Preskorn, *Current Psychiatry*, **10**, 84(2011)
12. J. Edwards, D. Chen, A. Ruth, M. E. Thase, *European Journal of Neuro Psychopharmocology*, **23**, S325(2013), http://dx.doi.org/10.1016%2FS0924-977X(13)70511-X
13. R. Jain, Chen, D. J. Edwards, M. Mathews, C*urrent Medical Research and Opinion,* **30,** 264(2013), https://doi.org/10.1185/03007995.2013.855188
14. Malcom M Campbell, Graham Johnson, *Chemical Rev*iews, **78**, 65(1978), https://doi.org/10.1021/cr60311a005
15. A. R. Vasudeva Murthy, B. Sanjiva Rao, *Proceedings of the Indian Academy of Sciences* **35**, 69(1952), https://doi.org/10.1007/BF03172477
16. A. Geethanjali, *Synlet,* **18**, 2857(2005), https://doi.org/10.1055/s-2005-918936
17. N. Sureshaan, D. KalyanRaj, *The International Research Journal of Pharm*acy, **8**, 62(2017), https://doi.org/10.7897/2230-8407.088146
18. S. Malini, K Raj, N. Suresh, K. S. Anantharaju, *Chemical Papers*, **76**, 1457(2022),

https://doi.org/10.1007/s11696-021-01934-y
19. M. S. Veena, M. K. Prashanth, K. Yogesh Kumar, *Journal of Chilean Chemical Society,* **60**, 3063(2015), http://dx.doi.org/10.4067/S0717-97072015000300019
20. Elizebath Choi, Monika Zmarlicka, J. Megan, M. J. Ehret, *American Journal of Health-System Pharmacy*, **69**, 1551(2012), https://doi.org/10.2146/ajhp110374
21. G. Rudrama Devi, G. Saravanan, Mohammad Yunoos, M. V. Sai Krishna, *Indian Journal of Research in Pharmacy and Biotechnology*, **5**, 164(2017)
22. K. Redasani Vivekkumar, F. Chhajed Chetan, D. Patil Pritam, J. Surana Sanjay, *Journal of Pharmaceutical Research*, **13**, 20(2014)
23. E. A. Molelwyn, J. Hughes, *Oxford University Press, London*, 297 (1947)
24. J. C. Morris, J. A. Salazarand, M. A. Wineman, *Journal of the American Chemical Society*, **70**, 203(1948), https://doi.org/10.1021/ja01186a016
25. E. Bishop, V. J. Jennings, *Talanta,* **1**, 198(1958), https://doi.org/10.1016/0039-9140(58)80034-X
26. F. E. Hardy, J. P. Johnston, *Journal of the Chemical Society Perkin Trans II,* **2**, 742(1973) https://doi.org/10.1039/P29730000742
27. F. G. Soper, G. F. Smith, *Journal of the Chemical Society*, 1582(1926), https://doi.org/10.1039/JR9262901582
28. S. Sriman Narayanan and V. R. S. Rao, *RadiochemActa,* **32**, 211(1983), https://doi.org/10.1524/ract.1983.32.4.211

[RJC-9230/2025]